

UDC 548.56:546.87:541.145

Haitao Liu¹, Baolin Yan², Chao Yang², Jikang Jian², A.B. Tateyeva³, Xintai Su²,
G.G. Baikenova³, M.I. Baikenov³, A. Satybaldin³

¹College of Physics Science and Technology, Xinjiang University, Urumqi, China;

²Ministry Key Laboratory of Oil and Gas Fine Chemicals,
College of Chemistry and Chemical Engineering, Xinjiang University, Urumqi, China;

³Ye.A. Buketov Karaganda State University, Kazakhstan
(E-mail: ualiev.a.84@mail.ru)

Solvothermal synthesis of BiOCl nanoplates with excellent photocatalytic activity for dye degradation

A two-phased solvothermal method was employed to synthesize BiOCl nanoplates using $\text{Bi}(\text{NO}_3)_3 \cdot 5\text{H}_2\text{O}$, sodium oleate and KCl as the starting materials. The phases, morphology and optical property of the products were characterized by X-ray powder diffraction (XRD), transmission electron microscopy (TEM) and UV-vis diffuse reflectance spectroscopy (DRS). XRD and TEM images showed that the BiOCl nanoplates have a tetragonal phase with the lateral length of 50–100 nm. DRS exhibited that the obtained BiOCl samples have great absorption in the ultraviolet light range. Methyl orange (MO) and Rhodamine B (RhB) were used as the target degradation to assess the photocatalytic properties of the samples. Under UV irradiation, the degradation rate of MO and RhB was reached to 96.3 % and 97.7 % within 30 min. The results indicated that the BiOCl nanoplates have great potential applications in dye degradation.

Keywords: BiOCl nanoplates, two-phased solvothermal method, photocatalytic, dye degradation.

1 Introduction

Water is essential to human life, industrial and agricultural production of natural resources. During the last few decades, the dye using caused serious environmental pollution, especially water pollution. Textile industry is rated as one of the most polluting sector among the different human activities due to their high discharge volume and effluent composition [1]. Solving the dye wastewater problem has become a hot topic of concern in the world. To date, semiconductor photocatalysis has attracted increasing attention as a potential environmental technology for wastewater remediation [2]. Photocatalysis is one of the most promising methods for environmental protection. It is friendly to the environments and has a relatively low cost. Thus, heterogeneous photocatalysts with high activities have attracted considerable interest

Recently, bismuth-based photocatalysts have received tremendous attention due to its unique layered structure that helps the separation of photo-generated electron-hole pairs [3]. Among them BiOCl as one of the most important bismuth oxyhalides, the predicted energy gap value is 3.3 eV, belongs to the indirect band gap semiconductor characteristic. In indirect bandgap semiconductor material, composite of electron-hole pairs can be conducted only by electron emission or absorption, which reduces the combination probability of photo generated electrons and holes [4]. Therefore, indirect jumps the characteristic and open style laminated structure at the same time exists is advantageous to the electron-hole effective separation and the electric charge transfer, causes that BiOCl have the good photochemical catalysis activity and the stability [5]. It has been revealed that the photocatalytic properties of BiOCl are not only related with the morphology but also synthetic methods. Various BiOCl nanostructures including nanobelts [6], nanowires [7], nanofibers [8],

nanoplates [9] and 3D hierarchical nanostructures [10, 11] have been fabricated via different synthetic routes, such as hydro/solvothermal method [12, 13], ionothermal synthesis [14], template-assisted synthesis [15], microwave-assisted synthesis [16] and hydrolytic synthesis [17, 18]. The prepared samples in terms of performance need further improvement, and the synthesis conditions are relatively harsh. In recent years, lamellar structure BiOCl materials have attracted much attention [19, 20]. Owing to its unique electronic, magnetic, optical, and catalytic properties, which mainly arise from their large surface areas [21]. Therefore, exploring a facile method to prepare BiOCl nanoplates structure with excellent photocatalytic activity for dye degradation is still desired.

In this paper, a two-phased solvothermal method was employed to synthesis BiOCl nanoplates. The photocatalytic activities of the as-prepared samples were evaluated by degradation of MO and RhB under UV light irradiation. The as-prepared BiOCl sample showed excellent photocatalytic activity for the degradation of MO and RhB, which was prepared without the presence of CTAB or NaOH. The degradation rate of MO and RhB was approached to 96.3 % and 97.7 % within 30 min under the same conditions. It is expected that the present study could be great potential value in photocatalytic activities.

2 Experimental

2.1 Preparation of photocatalyst

All of the reagents were analytical grade and were used as received. In a typical synthesis process, 2 mmol of $\text{Bi}(\text{NO}_3)_3 \cdot 5\text{H}_2\text{O}$ and 6 mmol of sodium oleate were put into 200 mL three-necked flask containing 15 mL of deionized water, 15 mL of ethanol and 30 mL of hexane. After stirred at room temperature for 1 h, the flask was moved into an oil bath and refluxed at a temperature of 70 °C for 30 minutes. Finally 4 mmol of KCl was added for heating backflow with stirring for 1 h. After cooled down to room-temperature, the mixture was transferred into a 25 mL capacity Teflonlined stainless steel autoclave, and kept at 180 °C for 12 h, and finally cooled to room temperature naturally. The product was washed with deionized water and ethanol for three times. The final products were then dried at room temperature for further characterization. This sample was denoted by BiOCl-1. For comparison, the BiOCl samples prepared by adding 6 mmol CTAB or NaOH with stirring of 30 min before the addition of KCl under the same conditions was denoted by BiOCl-2 and BiOCl-3, respectively. Another comparison sample was prepared by just refluxing for 2 h without the solvothermal treatment, which was denoted by BiOCl-4.

2.2 Characterization

The crystal structure of the samples was determined by X-ray diffraction (XRD, BRUKER D2 with Cu K_α radiation ($\lambda = 1.54178 \text{ \AA}$)). The microstructures of the samples were characterized by transmission electron microscopy (TEM, Hitachi H-600). The optical properties of the samples were tested by UV solid reaction instrument (Shimadzu UV-4802S PC).

2.3 Photocatalytic activity measurement

For photocatalytic measurement, take MO and RhB as the target degradation. 20 mg catalyst dissolved in 50 ml 10 mg/L MO and RhB solution respectively. Before the lighting, the suspensions were magnetically stirred in dark for 1 h in photochemical reaction apparatus (Xu Jiang machine plant in Nanjing XPA) to reach the adsorption-desorption equilibrium and then exposed to light from a 100 W Hg lamp. The suspension has been given time interval for liquid. Fetched suspensions was fed into a centrifuge tube, then placed the mixture in a centrifuge (Shanghai Anting Scientific Instrument Factory TCL-16C) in 10000 r/min centrifuged for 5 minutes to remove the catalysts. The suspensions were analyzed on a UV-vis spectrophotometer (Shimadzu UV-2550 PC) for testing analysis. The percentage of degradation is reported as C/C_0 , where C is the concentration of the dyes for each irradiated time, and C_0 is the starting concentration.

3 Result and discussion

3.1 XRD and TEM

Figure 1 showed the XRD patterns of the as-prepared samples. All of the diffraction peaks can be tallied with the standard card peaks of BiOCl (JCPDS card no. 06–0249) except the weak reflection of $\text{Bi}_4\text{O}_5\text{Cl}_2$ in the sample BiOCl-3. The peaks were narrow and strong, indicating that the as-prepared samples had good crystallinity. The XRD pattern of BiOCl-4 revealed a small amount of $\text{Bi}_4\text{O}_5\text{Cl}_2$ impurity.

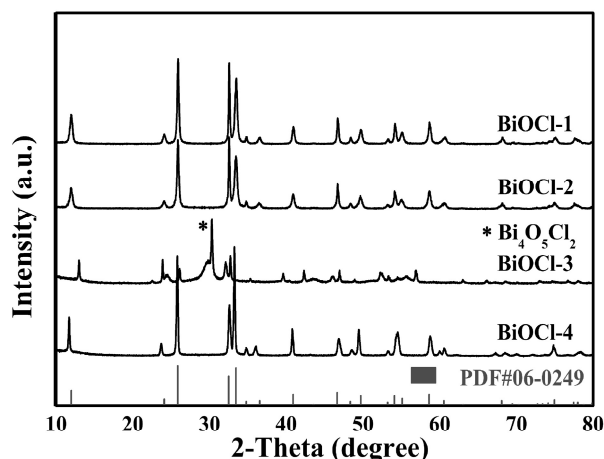
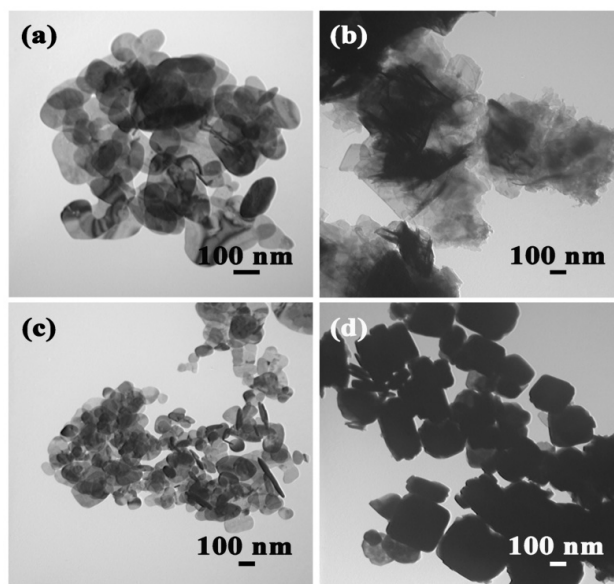


Figure 1. XRD patterns of BiOCl powder prepared at different conditions

Figure 2 showed the typical TEM images of the BiOCl samples. It is clearly observed that the samples consist of nearly regular sheets with a large distribution of 50–100 nm. As shown in Figure 2(a), BiOCl-1 has a clear sheet structure. This nanoplate dispersed well and there is no significant agglomeration. The sample BiOCl-2 shown in Figure 2(b), has larger sizes and serious agglomeration. Figure 2(c) showed BiOCl-3 nanoplate with a smaller size and obvious aggregation. BiOCl-4 (Fig. 2(d)) showed the morphology of the block structure. It can be concluded that BiOCl-1 has a more uniform particle size and better dispersion.



(a) — BiOCl-1; (b) — BiOCl-2; (c) — BiOCl-3; (d) — BiOCl-4

Figure 2. TEM images of BiOCl

Figure 3(a) showed the UV-vis diffuse reflectance spectra of the BiOCl samples. It can be seen that all the absorption peaks occurred at about 380 nm, which is consistent with the reported absorption edge of BiOCl [5]. Figure 3(b) is band gap of BiOCl samples, which was calculated by the following equation [22, 23].

$$\alpha h\nu = A(h\nu - E_g)^{n/2}, \quad (1)$$

Where α , ν , A and E_g represent the meaning of absorption coefficient, the frequency of the incident light, scaling factor and bandgap energy, respectively. Among them, the value of n depends on the type of semiconductor bandgap. The direct band gap semiconductor and indirect band gap semiconductor have different n value, and the value of n for indirect bandgap semiconductors is 4 [24, 25]. The band gap can be estimated by Tauc plot as shown in Figure 3(b). The band gaps of the as-prepared BiOCl samples were in the

range of 3.0 eV to 3.25 eV. Wherein, the band gap of BiOCl-1 was 3.25 eV. The BiOCl-1 sample exhibited wide ultraviolet absorption region and high light absorption, meaning that more electron-hole pairs can be produced under the UV irradiation, which would benefit its photocatalytic performance as shown below.

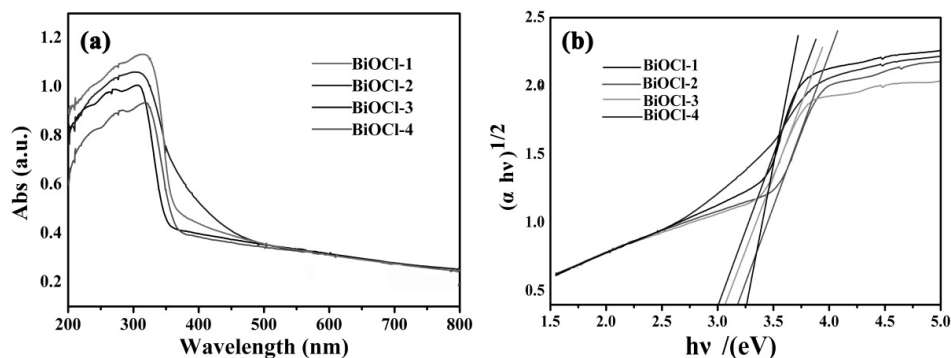


Figure 3. UV-vis diffuse reflectance spectra of BiOCl samples

3.2 Photocatalytic activity of BiOCl

The photocatalytic activities of as-synthesized BiOCl nano-plates have been evaluated by degradation of MO and RhB solution ultraviolet light irradiation. Figure 4 (*a–b*) shows the absorption spectra of MO and RhB solutions (10 mg/L) in the presence of BiOCl-1. The characteristic peak of MO at $\lambda = 463.5$ nm and RhB at $\lambda = 663$ nm weakened gradually along with the illumination time extension. When the illumination time was 30 min, the basic characteristic peaks were merely vanished. As a comparison, the photocatalytic activities of the other samples were checked under the same conditions. This indicated the as-prepared BiOCl has the excellent photochemical catalysis activity for both acid dyes and basic dyes. Figure 4(*c–d*) displayed the dye degeneration performance of BiOCl nanoplates prepared under different synthesis conditions. As showed in Figure 4(*c–d*), the dark adsorptions of MO and RhB were as low as 3 % and 9 %, respectively, showing almost no dye adsorption performance. When UV lamp was turned on, it was found that the sample of BiOCl-1 showed the highest catalytic activity among the samples and the degradation rate can reach to 96.3 % and 97.7 % within 30 min.

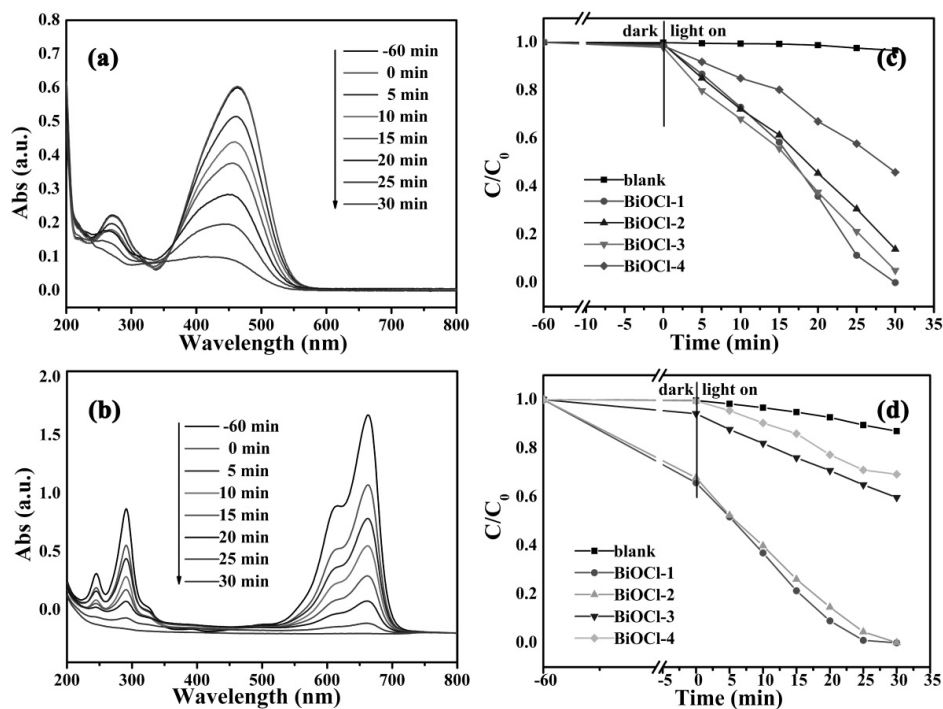


Figure 4. Spectral changes BiOCl-1 sample to ultraviolet MO and RhB solution absorption (*a–b*); BiOCl-1 sample for photocatalytic degradation of MO and RhB solution percentage (*c–d*)

4 Conclusions

In summary, the 2D sheet structure BiOCl nanoplates were synthesized through a two-phased solvothermal method. The lateral sizes of the nanoplates are in 50–100 nm range. The X-ray diffraction analysis indicates that the product is pure phase tetragonal BiOCl. The dye degradation experiment revealed its excellent catalytic performance for degradation of MO dye and RhB. The BiOCl nanoplates showed potential applications in the degradation of organic wastewater fields. This work provides a facile method for the synthesis of high photocatalytic activity BiOCl nanoplates.

References

- 1 Laet, J.De., & Le, T.G. (2006). Effects of chloride ions on the iron(III)-catalyzed decomposition of hydrogen peroxide and on the efficiency of the Fenton-like oxidation process. *Appl. Catal. B-Environ.*, *66*, 137–146.
- 2 Ye, L.Q., Deng, K.J., Xu, F., Tian, L.H., Peng, T.Y., & Zan, L. (2012). Increasing visible-light absorption for photocatalysis with black BiOCl. *Phys. Chem.*, *14*, 82–85.
- 3 Madhusudan, P., Ran, J.R., Zhang, J., Yu, J.G., & Liu, G. (2011). Novel urea assisted hydrothermal synthesis of hierarchical BiVO₄/Bi₂O₂CO₃ nanocomposites with enhanced visible-light photocatalytic activity. *Appl. Catal. B-Environ.*, *110*, 286–295.
- 4 Zhang, X.C., Zhao, L.J., Fan, C.M., Liang, Z.H., & Han, P.D. (2012). First-principles investigation of impurity concentration influence on bonding behavior, electronic structure and visible light absorption for Mn-doped BiOCl photocatalyst. *Physica B.*, *407*, 4416–4424.
- 5 Chang, X., Huang, J., Cheng, C., Sui, Q., Sha, W., & Ji, G., et al. (2010). BiOX (X= Cl, Br, I) photocatalysts prepared using NaBiO₃ as the Bi source: characterization and catalytic performance. *Catalysis Communications*, *11*, 460–464.
- 6 Deng, H., Wang, J.W., Peng, Q., Wang, X., & Li, Y.D. (2005). Controlled hydrothermal synthesis of bismuth oxyhalide nanobelts and nanotubes. *Chem.-Eur. J.*, *11*, 6519–6524.
- 7 Chen, C.C., Ma, W.H., & Zhao, J.C. (2010). Semiconductor-mediated photodegradation of pollutants under visible-light irradiation. *Chem. Soc. Rev.*, *39*, 4206–4219.
- 8 Peng, H.L., Chan, C.K., Meister, S., Zhang, X.F., & Cui, Y. (2009). Shape evolution of layer-structured bismuth oxychloride nanostructures via low-temperature chemical vapor transport. *Chem. Mat.*, *21*, 247–252.
- 9 Lu, Q.Y., Gao, F., & Komarneni, S. (2006). Cellulose-directed growth of selenium nanobelts in solution. *Chem. Mat.*, *18*, 159–163.
- 10 Ye, L.Q., Zan, L., Tian, L.H., Peng, T.Y., & Zhang, J.J. (2011). The {001} facets-dependent high photoactivity of BiOCl nanosheets. *Chem. Commun.*, *47*, 6951–6953.
- 11 Shang, M., Wang, W.Z., & Xu, H.L. (2009). New Bi₂WO₆ Nanocages with high visible-light-driven photocatalytic activities prepared in refluxing EG. *Cryst. growth Des.*, *9*, 991–996.
- 12 Zhang, K.L., Liu, C.M., Huang, F.Q., Zheng, C., & Wang, W.D. (2006). Study of the electronic structure and photocatalytic activity of the BiOCl photocatalyst. *Appl. Catal. B-Environ.*, *68*, 125–129.
- 13 Chai, S.Y., Kim, Y.J., Jung, M.H., Chakraborty, A.K., Jung, D., & Lee, W.I. (2009). Heterojunctioned BiOCl/Bi₂O₃, a new visible light photocatalyst. *J. Catal.*, *262*, 144–149.
- 14 Li, G.F., Ding, Y., Zhang, Y.F., Lu, Z., Sun, H.Z., & Chen, R. (2011). Microwave synthesis of BiPO₄ nanostructures and their morphology-dependent photocatalytic performances. *Journal. Colloid Interface Sci.*, *363*, 497–503.
- 15 Biswas, A., Das, R., Dey, C., Banerjee, R., & Poddar, P. (2014). Ligand-free one-step synthesis of {001} faceted semiconducting BiOCl single crystals and their photocatalytic activity. *Cryst. Growth Des.*, *14*, 236–239.
- 16 He, J., Wang, J., Liu, Y.Y., Mirza, Z.A., Zhao, C., & Xiao, W.Y. (2015). Microwave-assisted synthesis of BiOCl and its adsorption and photocatalytic activity. *Ceram. Int.*, *41*, 8028–8033.
- 17 Lin, H.X., Ding, L.Y., Pei, Z.X., Zhou, Y.G., Long, J.L., & Deng, W.H., et al. (2014). Au deposited BiOCl with different facets: On determination of the facet-induced transfer preference of charge carriers and the different plasmonic activity. *Appl. Catal. B-Environ.*, *160*, 98–105.
- 18 Xiao, X., Hao, R., Liang, M., Zuo, X.X., Nan, J.M., Li, L.S., & Zhang, W.D. (2012). One-pot solvothermal synthesis of three-dimensional (3D) BiOI/BiOCl composites with enhanced visible-light photocatalytic activities for the degradation of bisphenol-A. *J. Hazard. Mater.*, *233*, 122–130.
- 19 Osada, M., & Sasaki, T. (2012). Two-dimensional dielectric nanosheets: novel nanoelectronics from nanocrystal building blocks. *Adv. Mater.*, *24*, 210–228.
- 20 Park, K., Lee, J.S., Sung, M.Y., & Kim, S. (2002). Structural and optical properties of ZnO nanowires synthesized from ball-milled ZnO powders. *Jpn. J. Appl. Phys. Part 1 — Regul. Pap. Short Notes Rev. Pap.*, *41*, 7317–7321.
- 21 Deng, Z.T., Chen, D., Peng, B., & Tang, F.Q. (2008). From bulk metal Bi to two-dimensional well-crystallized BiOX (X = Cl, Br) micro- and nanostructures: Synthesis and characterization. *Cryst. Growth Des.*, *8*, 2995–3003.
- 22 Fujishima, A., & Honda, K. (1972). Electrochemical photolysis of water at a semiconductor electrode. *Nature*, *238*, 37–38.
- 23 Kim, H.W., Lee, J.W., & Shim, S.H. (2007). Study of Bi₂O₃ nanorods grown using the MOCVD technique. *Sens. Actuator B-Chem.*, *126*, 306–310.
- 24 Wang, Y., Shi, Z.Q., Fan, C.M., Hao, X.G., Ding, G.Y., & Wang, Y.F. (2012). Synthesis of BiOCl photocatalyst by a low-cost, simple hydrolytic technique and its excellent photocatalytic activity. *Int. J. Miner. Metall. Mater.*, *19*, 467–472.
- 25 Lin, H.L., Ye, H.F., Li, X., Cao, J., & Chen, S.F. (2014). Facile anion-exchange synthesis of BiOI/BiOBr composite with enhanced photo electrochemical and photocatalytic properties. *Ceram. Int.*, *40*, 9743–9750.

Хай Тау Лю, Бау Лин Иау, Шау Иан, Жи Кан Жиан, А.Б. Татеева,
Синтай Су, Г.Г. Байкенова, М.И. Байкенов, А. Сатыбалдин

Бояғыштардың деградациясына арналған жоғары фотокаталитикалық белсенді BiOCl нанобөлшектерінің сольвотермалды синтезі

Екіфазалы сольвотермалды әдіс бойынша BiOCl наноқабықшаларын синтездеу үшін бастапқы материал ретінде $\text{Bi}(\text{NO}_3)_3 \cdot 5\text{H}_2\text{O}$, натрий олеаты және KCl қолданылды. Туындылардың фазасын, морфологиясын және оптикалық қасиеттерін сипаттау үшін рентгендік ұнтақтық дифракция (XRD), электрондық микроскопия (TEM), ультракүлгін спектр аймағында (DRS) диффузиялық шағылыстыру спектроскопия пайданылды. XRD және TEM суреттері BiOCl наноқабықшаларының латералды ұзындығы 50–100 нм, пішіні тетрагоналды екенін көрсетті. BiOCl алынған үлгілері ультракүлгін сәуле аймағында жоғары сіңіру қабілетімен сипатталатынын DRS көрсетті. Үлгілердің фотокаталитикалық қасиеттерін бағалау үшін метилоранж (MO) және родамин В (RhB) қолданылды. Ультракүлгін сәулесінде MO және RhB деградациялау жылдамдығы 96,3 % и 97,7 % дейін 30 мин аралығында жоғарлады. Қорытынды нәтижесі бояуды азайту барысында BiOCl нанобөлшектердің әлеуетті қолдану аймағы артатындығын көрсетті.

Кілт сөздер: BiOCl наноқабықшалар, екіфазалы сольвотермалды әдіс, фотокаталитикалық қасиеттер, құлдырау.

Хай Тау Лю, Бау Лин Иау, Шау Иан, Жи Кан Жиан, А.Б. Татеева,
Синтай Су, Г.Г. Байкенова, М.И. Байкенов, А. Сатыбалдин

Сольвотермальный синтез нанопластинок BiOCl с высокой фотокаталитической активностью для деградации красителей

Для синтеза нанопластинок BiOCl использовали двухфазный сольвотермальный метод с применением в качестве исходных материалов $\text{Bi}(\text{NO}_3)_3 \cdot 5\text{H}_2\text{O}$, олеата натрия и KCl. Фазы, морфология и оптические свойства продуктов характеризовались методами рентгеновской порошковой дифракции (XRD), просвечивающей электронной микроскопии (TEM) и спектроскопии диффузного отражения в УФ-видимой области спектра (DRS). Изображения XRD и TEM показали, что нанопластины BiOCl имеют тетрагональную фазу с латеральной длиной 50–100 нм. DRS показал, что полученные образцы BiOCl обладают большим поглощением в диапазоне ультрафиолетового света. Для оценки фотокаталитических свойств образцов для деградации использовали красители метиловый оранжевый (MO) и родамин В (RhB). При УФ-облучении скорость деградации MO и RhB достигала 96,3 % и 97,7 % в течение 30 мин. Результаты показали, что нанопластины BiOCl имеют большой потенциал для деградации красителей при их применении.

Ключевые слова: нанопластины BiOCl, двухфазный сольвотермальный метод, фотокаталитические свойства, деградация.